

See discussions, stats, and author profiles for this publication at: <https://www.researchgate.net/publication/51179107>

Probing Multivalent Host–Guest Interactions between Modified Polymer Layers by Direct Force Measurement

ARTICLE *in* THE JOURNAL OF PHYSICAL CHEMISTRY B · JUNE 2011

Impact Factor: 3.3 · DOI: 10.1021/jp110939c · Source: PubMed

CITATIONS

9

READS

28

6 AUTHORS, INCLUDING:



Oznur Kaftan

University of Bayreuth

5 PUBLICATIONS 89 CITATIONS

SEE PROFILE



Frederic Dubreuil

University of Grenoble

28 PUBLICATIONS 1,108 CITATIONS

SEE PROFILE



Andreas Fery

Leibniz Institute of Polymer Research Dresden

251 PUBLICATIONS 4,840 CITATIONS

SEE PROFILE



Georg Papastavrou

University of Bayreuth

53 PUBLICATIONS 1,241 CITATIONS

SEE PROFILE


Probing Multivalent Host–Guest Interactions between Modified Polymer Layers by Direct Force Measurement

Oznur Kaftan,[†] Simonetta Tumbiolo,[‡] Frédéric Dubreuil,[§] Rachel Auzély-Velty,[§] Andreas Fery,^{*,†} and Georg Papastavrou^{*,†}

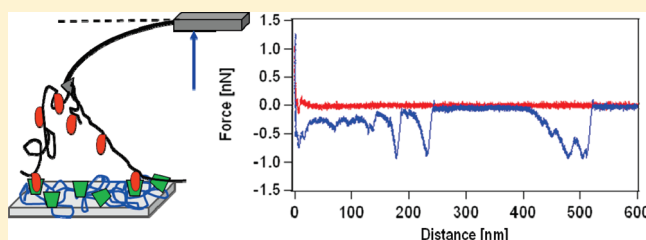
[†]Department of Physical Chemistry II, University of Bayreuth, Universitätsstrasse 30, 95440 Bayreuth, Germany

[‡]Department of Inorganic, Analytical, and Applied Chemistry, University of Geneva, Sciences II, 30, Quai Ernest-Ansermet 1211 Geneva 4, Switzerland

[§]Centre de Recherches sur les Macromolécules Végétales, CNRS, affiliated with Université Joseph Fourier, BP 53, 38041 Grenoble Cedex 9, France

 Supporting Information

ABSTRACT: The adhesion behavior between modified polysaccharide layers capable of forming host–guest complexes has been determined by direct force measurements with the atomic force microscope (AFM). Polysaccharides bearing either host or guest moieties were obtained by derivatization of chitosan with pendant β -cyclodextrin (CD) and adamantane (AD) moieties, respectively. These modified polysaccharides were covalently immobilized either to flat surfaces or to AFM-probes. The number of interacting polymer segments has been reduced significantly by covalently immobilizing chitosan to an AFM-tip with small radius and measuring the forces between the protruding polymer segments and a chitosan layer immobilized to a flat surface. By this approach, it was possible to determine the interaction between polymer layers on the level of single polymer strands. To separate contributions to the adhesion due to the formation of host–guest complexes from unspecific interactions, we performed measurements between various combinations of chitosan derivatives. With the same polymer probe of adamantane-modified chitosan, the interaction against a number of different chitosan layers has been determined, including ones that are not able to form host–guest complexes, such as unmodified chitosan or β -cyclodextrin modified chitosan, which has been blocked previously by addition of adamantane. The resulting adhesion behavior has been analyzed in terms of the total work of adhesion, the number of rupture events, and the corresponding lengths of the polymer segments as well as rupture forces. A clear difference has been found for systems where the formation of host–guest complexes is possible in comparison to the absence of specific multivalent interaction between the polysaccharide layers. In particular, the work of adhesion is increasing up to an order of magnitude upon the formation of host–guest complexes between the chitosan layers.



INTRODUCTION

Biological systems are able to form highly complex and well-defined structures with several hierarchical levels on the basis of noncovalent bonds. Mimicking such self-assembly processes in artificial systems represents an important step toward the construction of novel intelligent and adaptable materials. The specific recognition provided by a receptor/ligand combination represents in biological systems the most common and versatile principle to form ordered structures. Therefore, the introduction of receptor–ligand systems as “connectors” for different building blocks received much attention also for building-up artificial structures. Recent applications include stimuli-sensitive hydrogels,^{1,2} selective bilayer vesicles,^{3,4} polymeric films based on multilayer structures,^{5,6} and 2D or 3D nanostructures based on “molecular printboards”.^{7,8} However, more complicated structures with a higher degree of order have been obtained by combining synthetic supramolecular elements with biomolecules.⁹

These applications are based on the formation of multiple host–guest complexes, often in combination with polymeric systems.

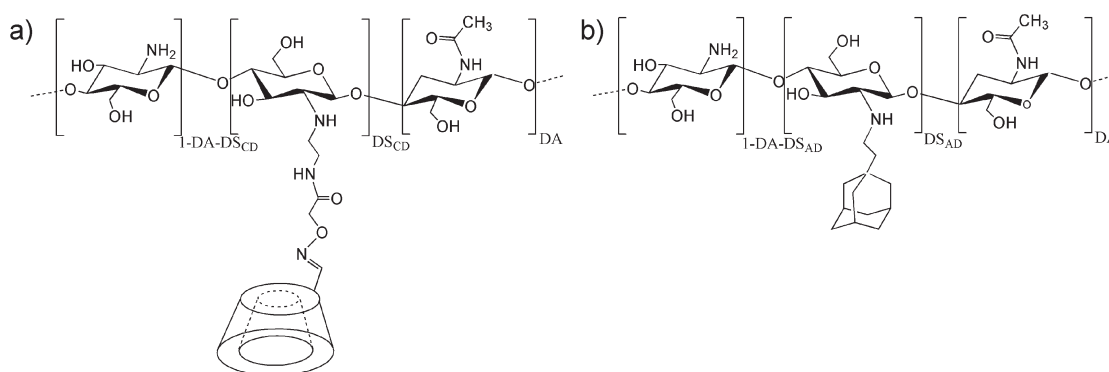
The underlying concept of multivalency, that is, multiple bonds that are formed sequentially or simultaneously, is of great importance to design and optimize the single building blocks, as well as to optimize the parameters for their assembly.¹⁰ Combined with a suitable thermodynamic and kinetic behavior, the multiple interactions between a large ensemble of functionalities provide a tunable directional pathway for the self-assembly of stable synthetic materials structured by supramolecular interactions. However, the physical chemistry of these systems, especially if they are of polymeric origin, is considerably more complex than that of single host–guest systems. Despite the importance of multivalency, in particular for biological systems, it attracted only recently wider interest.^{11,12} However, multivalency has been mostly studied in relation to bulk materials.¹³ Only recently, the effect of multivalency of host–guest

Received: November 16, 2010

Revised: April 19, 2011

Published: May 31, 2011

Scheme 1. Chemical Structures of the Modified Chitosans: (a) Chitosan with Grafted β -Cyclodextrin (CHI-CD) and (b) Chitosan with Grafted Adamantane



interaction at polymeric interfaces has been reported in a number of theoretical and experimental studies.^{14–16}

The binding characteristics of single host–guest complexes have been studied extensively. In this respect, interactions at interfaces were often of particular interest, motivated, for example, by applications in sensor technology.^{17,18} With the advent of single molecule force spectroscopy, either based on the atomic force microscope (AFM) or optical/magnetic tweezers, it became possible to probe directly the unbinding of a single ligand–receptor pair under an external force.^{19–23} By using flexible linkers, steric freedom for the formation of complexes is obtained, and surface contributions are reduced.^{23–25} Besides numerous studies focusing entirely on biologically relevant receptor–ligand systems, also molecular building blocks allowing for inclusion complexation, host–guest interactions, have been studied by force spectroscopy with the AFM.^{26,27} The interaction forces between bare polymer layers have also been studied extensively by direct force measurements, in particular, the resulting adhesion behavior.^{28–33} However, the interaction forces between polymeric layers bearing moieties for specific binding have been considered only very recently.³⁴ The information provided by direct force measurements on such systems is highly relevant for many applications to better understand how the polymers adhere on different surfaces by specific short-range interactions and how polymer–polymer interactions can be controlled within the polymer layers by polyvalent chemical interactions. These results would be important for many applications, such as controlled and directed adhesion of polymer-coated materials on surfaces or the self-assembly of polymers with layer-by-layer (LbL) technique to obtain multilayers with additional functionality.^{5,35}

In this study, we focus on determining the interaction forces between chitosan layers bearing additional functionality. Chitosan has been modified by grafting β -cyclodextrin (CD) and adamantane (AD) moieties, respectively, thereby allowing for host–guest interaction between the two polysaccharide layers. The CD acts as host molecule and AD acts as guest molecule. Chitosan is a natural polysaccharide and consists of *N*-acetyl-glucosamine and *N*-glucosamine units. It is derived by alkaline deacetylation of chitin, which is present, for example, in shellfish.³⁶ Chitosan is a weak polyelectrolyte and has a rather high intrinsic persistence length due to its saccharide units.^{37–39} Chitosan has found many applications in pharmacology, drug delivery, and tissue-engineering due to its biocompatibility, biodegradability, antimicrobial, and wound-healing activity.⁴⁰

Inclusion host–guest complexes formed by CD and hydrophobic AD are known for their relatively high binding energy on the order of about 20 kT.⁴¹ The high binding affinity and its steric selectivity with regard to the small size of the host–guest moieties make this host–guest system very effective not only to control the adhesion with solid substrates but also to tune the interaction between different chitosan strands. In contrast to biological receptor–ligand pairs, which show a pronounced rate dependence described by the Evans–Bell theory,^{42,43} many supramolecular systems show fast (un)binding kinetics and therefore no pronounced rate dependence. In particular, the combination of β -cyclodextrin and adamantane belongs to the latter class of specific interactions, as demonstrated by direct force measurements.^{26,27}

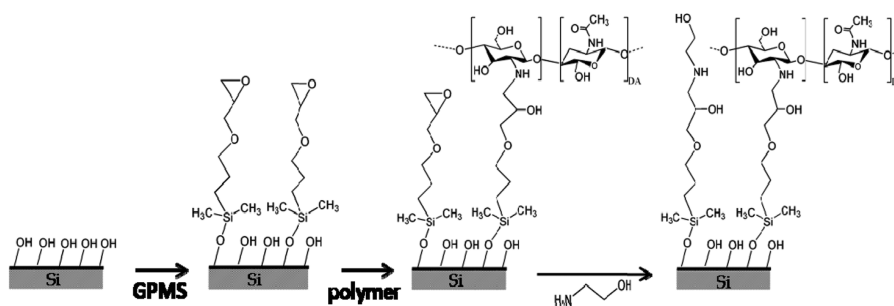
The number of interacting polymer segments has been reduced significantly as compared to colloidal probe studies by the direct immobilization of chitosan to AFM-tips with a small tip-radius. The interaction between the chitosan segments protruding from the tip and the chitosan layer immobilized on a flat surface was measured by AFM force spectroscopy. This approach resembles the one utilized in determining the desorption force of single polymer chains from a solid substrate.^{44–46} However, in the here-presented study both surfaces are of polymeric origin. Thus, the interaction between two polymer segments is measured rather than the interaction between a polymer and a flat solid substrate. The resulting force profiles are analyzed in a quantitative manner to separate the influence of the host–guest complexes from the interaction of the bare polysaccharides.

MATERIALS AND METHODS

Materials. 3-(Glycidioxypropyl)-dimethylethoxysilane (GPMS) has been purchased from ABCR (Karlsruhe, Germany). Ultrapure chitosan (PROTASAN UP B 80/500) with a degree of acetylation of about 9% was purchased from Novamatrix (Oslo, Norway). The molecular weight of the polymer with 372,000 Da has been determined by size exclusion chromatography. The β -cyclodextrin was kindly provided by Roquette Frères (Lesterm, France). 1-Adamantaneethanol, 1-adamantanecarboxylic acid (AD-COOH), and ethanolamine were obtained from Aldrich. All other chemicals and solvents were purchased from Sigma-Aldrich and have been used without further purification.

Modification of Chitosan. The synthesis of β -cyclodextrin (CD) and adamantane (AD) grafted chitosans (CHI-CD and CHI-AD) has been described in detail previously.^{47–49} The

Scheme 2. Schematic Representation of the Immobilization Steps of Modified Chitosans on the Silicon Wafer Substrates and Silicon Cantilevers



procedure used in this study has been slightly modified and is described in the following. The monosubstituted CD functionality is synthesized in three steps.⁴⁹ First, the bare CD is oxidized to its aldehyde with Dess–Martin periodinane according to a Dess–Martin reaction. Second, the oxidized CD is reacted with *O*-(carboxymethyl)-hydroxylamine hemihydrochloride to obtain mono-, di-, and tricarboxylic acid derivatives of CD. To obtain the monofunctionalized CD for grafting to the chitosan, the mixture of the carboxylic acid derivatives was fractionated by size exclusion chromatography on a Biogel (Bio-Rad, USA) P-4 column (4×100 cm) with NaNO₃. The monocarboxylic acid derivative of CD was then purified by diafiltration with deionized water through an ultramembrane (Amicon YC05, Millipore). Third, the monocarboxylic acid derivative of CD was reacted with aminoacetaldehyde dimethyl acetal to have protected aldehyde groups, which can be easily deprotected at acidic conditions. Similarly, to convert the hydroxyl groups to highly reactive aldehyde functional groups, the 1-adamantaneethanol was oxidized to adamantane acetaldehyde as described previously.⁴⁷ Oxidation was performed with pyridinium dichromate, and then the product was purified by silica gel chromatography.

The aldehyde derivatives of CD and AD, respectively, were grafted to chitosan by a reductive amination reaction between the primary amine groups present on the chitosan and the aldehyde groups on the derivatized host or guest molecules.^{49,50} The chemical structures of the modified chitosans (CHIs) are given in Scheme 1. Aldehyde modification and the attachment of the CDs were performed on the secondary rim to provide free access of the complementary AD-units. The introduction of a guest molecule in the CD-cavity takes normally place from the wider primary rim side, which contains secondary hydroxyl groups.

The degree of substitution for both modified CHIs was calculated as 0.08 (i.e., on average, one CD/AD every 12 glucosamine units) from digital integration of the NMR signals resulting from the anomeric protons of chitosan and CD as well as the protons of AD.^{47,51} The molecular mass after modification has been determined by capillary viscometry with an Ubbelohde capillary viscometer (Schott, Germany) attached to a Schott AVS 360 digital counter (Schott, Germany) at 25 °C. The viscometric average molecular weights M_v have been calculated according to the Mark–Houwink equation.⁵² We obtained M_v -values for unmodified CHI of 246 kDa, and for the modified chitosans of 270 kDa (CHI-CD) and 333 kDa (CHI-AD), respectively. On the basis of the degree of acetylation and the degree of substitution, one can expect approximately ~ 180 CD or AD units per chain to be present per chitosan molecule. This corresponds to an average distance

of ~ 14 nm between the AD or CD units, assuming a homogeneous distribution.

Silane Modification of Surfaces and AFM-Cantilevers. Flat substrates were prepared from silicon wafers (ABC, Munich, Germany). After being cut, they were cleaned by a modified RCA-cleaning procedure.⁵³ The substrates were first sonicated in a 3:1 (v/v) isopropanol/water mixture for 15 min in an ultrasonic bath. Next, the substrates were rinsed with Milli-Q water and treated in a mixture (v/v/v = 5:1:1) of deionized water, ammonia (25 vol %), and hydrogen peroxide (35 vol %) at 75 °C for 20 min. Afterward, they were rinsed with Milli-Q water and dried by a nitrogen stream. Silanization by GPMS was carried out from the gas phase by placing the samples inside a dry-seal desiccator containing 500 μ L of the silane. After application of vacuum for 30 min, the samples were kept in the desiccator for 24 h at room temperature. Afterward, the substrates were thoroughly rinsed with ethanol to remove all noncovalently bound silane and dried by a nitrogen stream.

The modification of AFM-tips was carried out analogously to that of the substrates. Here, we used contact-mode cantilevers made from silicon without any reflective coatings (CONT, Nanosensors, Wetzlar, Germany). These cantilevers have a length of 450 μ m, width of 50 μ m, and a nominal spring constant of 0.2 N/m. The only difference to the treatment described above was that the RCA-cleaning has been replaced by plasma treatment with an air plasma for 4 min (35 W, PDC-32G from HarriK Instruments).

Covalent Attachment of Chitosan. The coupling of modified chitosans to the modified substrates and the AFM-cantilevers was performed overnight at room temperature, in a solution of 0.5 g L⁻¹ CHI-CD (or CHI-AD) dissolved and stirred for 12 h in 0.3 M acetic acid. Grafted substrates were then sonicated in Milli-Q water for 3 min, rinsed intensively, and dried under a nitrogen stream. AFM-tips were just thoroughly rinsed with Milli-Q water and dried by a nitrogen stream. To achieve full quenching of any excess epoxy groups, the silica wafers and AFM cantilevers were placed for 30 min in a 2% aqueous ethanolamine solution, then rinsed with milli-Q water and kept in measurement buffer until the start of the measurements. The surface modification chitosan immobilization is schematically represented in Scheme 2.

Surface Characterization. Three different techniques have been used to characterize the surface before and after surface modification: (a) contact angle measurements, (b) ellipsometry, and (c) topographic imaging by atomic force microscopy. In detail, the surfaces have been examined in the following way: (a) Static water contact angle measurements were performed using the Contact Angle Systems OCA-15 (DataPhysics, Filderstadt,

Germany). A deionized water droplet ($\sim 25 \mu\text{L}$) was deposited to the surface and then imaged by a 50 mm objective mounted on a slow-scan CCD camera. An image analysis software SCA-20 package was used to determine the contact angle from the image. (b) Ellipsometric measurements were performed by Null ellipsometry at an incident angle of 70° with a helium–neon laser source ($\lambda = 633 \text{ nm}$) on a Multiskop (Optrel, Berlin, Germany). All measurements were conducted in air at room temperature. Oxide layer thickness for freshly cleaned Si-wafer was calculated by the MATLAB program using a two-layer model with uniform refractive indices of $3.85 + 0.02i$ and 1.46 for the silicon base and silicon oxide layer, respectively. Film thicknesses after modification by GPMS and immobilization of the chitosan layers were calculated using a multilayer model with uniform refractive index of 1.50 and 1.58 for the silane and chitosan layers, respectively.⁵⁴ (c) AFM images of the modified surfaces were obtained in tapping mode in air. The AFM for imaging was a Multimode equipped with a Nanoscope IIIa-controller (Veeco, Santa Barbara, CA). Standard tapping cantilevers (OMCL-AC160TS, Olympus) have been used for AFM-imaging purposes.

Direct Force Measurements. The interaction forces between a chitosan-modified AFM-tip and a flat surface have been measured with a dedicated AFM (MFP-3D, Asylum Research, Santa Barbara). The spring constants of the cantilevers were determined by the thermal noise method.⁵⁵ The thereby obtained spring constant was verified by method of Sader,⁵⁶ and both values were found to agree within 10–20%. It has to be pointed out that only one cantilever was used for each set of data, which comprises the interaction of one polymer probe against various different chitosan derivatives. The polymer attachment results in a specific distribution of polymer segments on the tip and leads therefore to a unique distribution of detachment and unbinding events.

All measurements were performed in acetate buffer at pH 3.7 (CH_3COOH 0.3 M/ CH_3COONa 0.03 M) and at room temperature. If not otherwise stated, the force curves were acquired at a frequency of 0.5 Hz, leading to approach and retraction velocities of about $0.6 \mu\text{m s}^{-1}$. The maximum loading force against the substrate after the contact of the probe was below 1.7 nN. Force distance curves were collected from 5 different positions on the substrate, and about 100 force curves were measured at each position.

RESULTS AND DISCUSSION

The interaction between polysaccharide layers bearing host–guest complexes is studied in this work by force spectroscopy with the AFM. To follow the interaction on the level of single polysaccharides, we utilized a new approach for the direct force measurements: A sharp AFM-tip is modified in such a manner that only a small number of polysaccharide strands protrude from it. These polymer strands are brought into contact with a polysaccharide film, which is covalently immobilized to a flat substrate. By force spectroscopy, the stretching of the single polysaccharide strands and the detachments as well as unbinding events following the separation of the AFM-tip from the surface are followed. This approach is similar to the one employed for studying the polymer desorption from flat surfaces.^{44–46} Here instead, the interaction between polymer strands is probed rather than desorption of a polymer chain from a flat surface.

Chemical Modification of Chitosan and Its Immobilization. The CD moieties were monosubstituted and bound from the secondary rim to the chitosan backbone to provide free access of

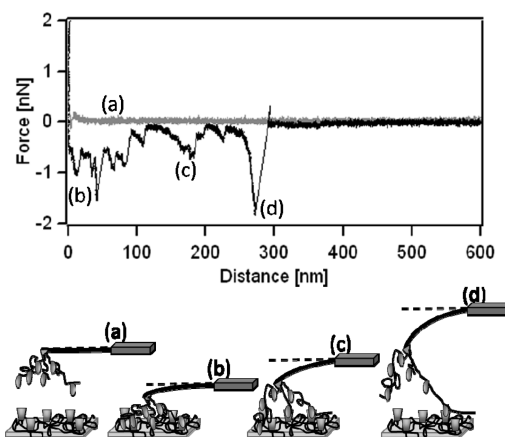


Figure 1. A typical force profile for approach and separation of two surfaces with covalently immobilized, modified chitosan strands. The combination of CHI-AD (polymer probe) and CHI-CD (flat surface) leads to a large number of detachment events upon separation of the polymer probe from the surface due to the formation of host–guest complexes. This process is depicted in a schematic manner in the lower part of the figure.

the complementary AD-units (cf., Scheme 1). Secondary rim monosubstituted CDs demonstrate the same recognition properties as unmodified ones for small guest molecules in solution^{47,50} or at solid interfaces of self-assembled monolayers.^{57,58}

The covalent immobilization of chitosan, either in its modified (CHI-CD) or unmodified form (CHI), was performed in two steps. First, the silicon substrates were coated with a silane layer of (3-glycidioxypropyl)dimethylethoxysilane (GPMS) terminating in epoxide groups.^{59–61} The formation of a monolayer was ensured by choosing a monoethoxy-silane.⁶² The GPMS layer thickness was determined as $5.0 \pm 1.3 \text{ \AA}$ by ellipsometry. This value is in agreement with the value $8.5 \pm 1.5 \text{ \AA}$ reported for a similar silane.^{59,63} The measured contact angle for water drop was $60^\circ \pm 3^\circ$ after modification by GPMS, again in agreement with the $55 \pm 10^\circ$ reported for a comparable silane.⁶³ Second, chitosan was covalently immobilized to the GPMS layer. The resulting layer in the dried state has an average thickness of $1.2 \pm 0.5 \text{ nm}$ (CHI-CD) and $1.1 \pm 0.1 \text{ nm}$ (CHI), respectively, as determined by ellipsometry. The average contact angle of chitosan grafted surface was $39^\circ \pm 2^\circ$ (CHI-CD) and $43^\circ \pm 2^\circ$ (CHI), respectively. The surface topography determined by tapping mode AFM indicates a high coverage of surface by chitosan in the dried state. Only on the large scale can the samples be considered as homogeneous. On the level of 30–50 nm, the samples show the structure of single polysaccharide globules, similar to layers obtained by the physisorption of polyelectrolytes or polysaccharides at higher ionic strength.^{32,33} Despite the covalent immobilization technique utilized, the film ultrastructure and its thickness resemble that of physisorbed polysaccharide films.⁶⁴

The preparation of chitosan-modified AFM-probes with a nominal tip radius of 10–20 nm has been performed analogously. In the following, we will refer to these polysaccharides-modified AFM-tips as polymer probes, and a schematic representation of these probes is given in the lower part of Figure 1.

Force Profiles of Chitosan-Adamantane Probe versus Chitosan-Cyclodextrin Layer. Figure 1 shows a typical force profile obtained between a CHI-AD polymer probe interacting with a CHI-CD layer immobilized to a flat substrate. The force

profile represents the interaction forces upon approach (gray) and retraction (black) as a function of the separation distance between the surfaces. The data have been acquired in an acetate buffer of pH 3.7 and of a total ionic strength of 0.03 M. In the following, we will shortly discuss the force versus distance profile for the approach and retraction part in a qualitative manner. For the interaction of CHI-AD versus CHI-CD, the formation of host–guest complexes is expected.

Upon approach of the polymer probe to the sample surface, no interaction forces can be detected at large separation distances (cf., Figure 1a). With decreasing distances, a small repulsive force occurs at separations of 10–50 nm. This force is varying in magnitude with the lateral position of the sample. These repulsive forces result primarily from steric forces due to the compression of the polysaccharide strands protruding in the solution. Steric forces can be approximated to a good degree of accuracy by an exponential force profile.⁶⁵ The values for the corresponding decay constants extrapolated from the force profiles would indicate values for the ionic strength 2–3 orders of magnitude lower than the ones expected on the basis of the solution composition of the acetate buffer. Such deviation is an indication for the domination of steric interactions over electrostatic interactions, where instead the decay constant would correspond to the Debye length for a given ionic strength.³² Only at small separation distances (i.e., below ~10 nm) does the bridging of the polymer strands lead in some cases to a jump of the cantilever to the surface due to attractive forces. Upon contact the tip is pressed against the surface up to a defined maximum loading force of approximately 1.7 nN. After reaching the maximal force, the two surfaces remain in contact for a defined time interval. During this so-called dwell time, which is here about 4 s, the modified chitosan strands can rearrange at the interface and thus interact to form host–guest complexes. Finally, the direction of the piezo movement is reversed, and the polymer probe is retracted from the surface (cf., Figure 1b).

The adhesion between the polymer strands is probed during the retraction part of the force profile (black data points in Figure 1). For the combination of a CHI-AD polymer probe and a surface coated by CHI-CD, one detects a large number of adhesion events. The majority of these events is occurring at large separations between sample and probe. It is essential to point out that more than one polysaccharide strand protrudes from the polymer probe. Thus, multiple stretching and rupture events are common for the retraction part of the force profiles. These events follow a common pattern: In the beginning, a nonlinear force versus extension behavior occurs, which is characteristic for the stretching of synthetic polymers or polysaccharides.^{66,67} Finally, the restoring force of the AFM-cantilever overcomes the binding forces between these polysaccharide strands or the surface. The sudden detachment leads to an instability in the force curves, where the cantilever suddenly returns to a less deflected state as the polymer strands detach. For all force profiles of the combination CHI-AD/CHI-CD, this pattern repeats many times due to the large number of host–guest complexes, which can be formed by one chitosan segment and the possibility of simultaneously bridging and thus stretching more than one polysaccharide strand. (cf., Figure 1c and d). Similar force curves upon retraction have been observed for the adhesion between like-charged polyelectrolyte layers, where bridging occurs between the polyelectrolytes and the opposing surfaces.^{31,32,68} For host–guest systems attached to long polymeric spacers, comparable patterns have also been reported.^{17,24,25} A quantitative analysis of the force profiles follows in the next paragraphs.

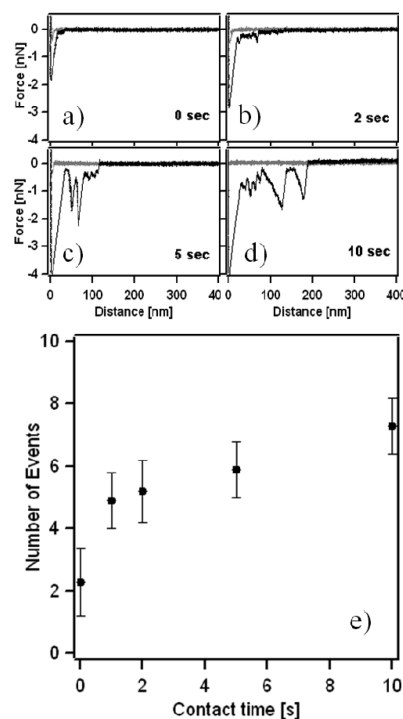


Figure 2. Representative force profiles obtained by varying the contact time for a CHI-AD polymer probe and a CHI-CD layer (a–d). The number of events as a function of contact time is shown in the bottom part of the figure (e).

Influence of Contact Time. Supramolecular interactions, such as the formation of host–guest complexes, are short-ranged.¹² Thus, spatial vicinity and appropriate orientation of the host and guest molecules are prerequisites for the formation of an AD/CD-complex. In consequence, the number of binding events between CHI-AD and CHI-CD depends on the relative orientation of the polymer strands. The number of formed complexes should increase with the time available for reorientation and then level off when all possible host–guest complexes have been formed. To prove this assumption, we varied systematically the so-called dwell time, which is defined as the time that the tip remains in contact with the surface after reaching maximum loading force. The total contact time is then given by the sum of this dwell time and the time the tip is in contact with the surface while the z-piezo element is moving, which corresponds in our experiments to approximately 0.1 s.

Figure 2 shows a set of representative force profiles acquired with increasing contact times (0.1–10.1 s) but constant maximum load forces. Additionally, the average number of rupture events detected upon separation of the surfaces is plotted versus the contact time. The force profiles demonstrate that the number of events is strongly related to the contact time: For a contact time of 0.1 s (cf., Figure 2a), only one or two rupture events are occurring. Instead, for contact times larger than 5 s, one finds more than five events (cf., Figure 2c,d). Additionally, most of these events are occurring at large separation distances. These qualitative trends are confirmed by quantitative analysis, where the number of detachment events has been determined. Figure 2e plots the number of events against the total contact time. For each contact time, more than 300 curves have been evaluated, and the error bars represent the corresponding standard deviations. Indeed, after a first rapid increase in the number of events, the total event number levels off for contact times larger than 5 s. Such

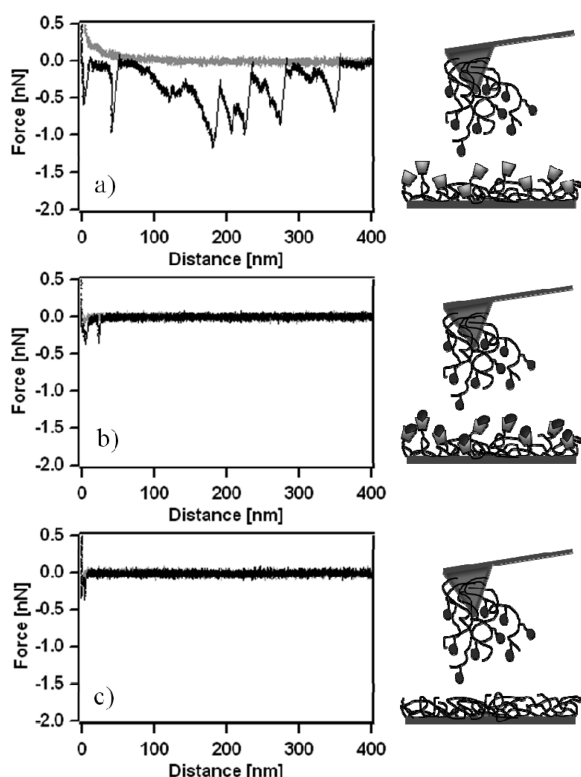


Figure 3. Representative force–distance profiles measured with the same chitosan–adamantane polymer probe (CHI-AD) versus samples bearing (a) a CHI-CD layer surface, (b) a CHI-CDBlocked layer in which the hosts (CD) were rendered inaccessible by previous incubation with AD, and (c) a CHI-layer.

a behavior is expected due to the rearrangement of the polymer chains protruding from the probe, because with increasing contact time a larger number of conformations of the polysaccharide strands and also a larger area of the sample can be probed, which favors the formation of more host–guest complexes between CD and AD moieties. Based on Figure 2e, all data presented in the following were obtained for contact times of approximately 4 s. This time interval provides sufficient time for the arrangement of the polymer strands but is also short enough to allow for the acquisition of a statistically relevant number of force profiles at different positions of the sample. It should be pointed out that the average number of events per curve is not only a function of the contact time but also of the number and length of polymer chains protruding from the polymer probe. However, the same trends are found for different polymer probes prepared in the same manner.

Specificity of Host–Guest Interactions. Many host–guest interactions are highly specific, in difference to other interactions taking place between polymer layers, such as intercalation/entanglement or hydrophobic and electrostatic interactions. To separate the contributions due to the formation of CD/AD-complexes from these nonspecific contributions, we compared the adhesion of the same polymer probe (CHI-AD) with various surfaces including those where no host–guest interaction is possible. The latter surfaces were prepared either by immobilizing bare, unmodified chitosan to flat surfaces or by blocking the cyclodextrin-hosts (CD) entities directly before the measurement (CHI-CDBlocked). Such blocking can be obtained by incubation in a solution containing 1 mM 1-adamantanecarboxylic

acid (AD-COOH) at pH 8 for 20 min before transferring the sample to the acetate buffer solution (pH 3.7), which contains no adamantane.

Figure 3 shows representative force profiles obtained with the same polymer probe (CHI-AD) but different chitosan derivatives as sample. All measurements have been performed under identical conditions (maximum load force, contact time) in the same buffer solution. Figure 3a shows a force profile for the interaction of the polymer probe with a chitosan layer bearing β -cyclodextrin moieties (CHI-CD) at the surface. The formation of the host–guest complexes leads to a large number of rupture events with the corresponding stretching of polysaccharide segments. Instead, blocking on the same sample the CD-moieties by a short incubation in AD-COOH leads to very different force profiles upon separation of the surfaces as shown in Figure 3b. For the blocked surfaces, CHI-CDBlocked, the adhesion is significantly reduced. Not only is the number of rupture events strongly reduced, but these events are also occurring closer to the sample surface. However, if this sample is exchanged with a fresh, unblocked sample bearing CHI-CD, the same adhesion profile as shown in Figure 3a is found again (see the Supporting Information). Different from comparable studies, no AD-COOH has been added to the solution in which the measurements CHI-AD versus CHI-CDBlocked have been carried out.²⁷ This approach has been chosen to be able to measure under the same buffer conditions as for the other samples. The equilibrium constant of the AD/CD complex is relatively high and lies in the order of $1–10 \times 10^4 \text{ M}^{-1}$.^{69–71} Therefore, dissociation in the time scale of the experiments is possible. However, the low solubility of AD-COOH under acidic conditions⁷² is supposed to have a significant influence in reducing such dissociation upon change of the solution conditions. The influence of pH on the equilibrium constant of AD-COOH has been described previously.⁶⁹ As the CHI-CD layer is covalently immobilized to the surface, we believe that secondary effects, such as irreversible conformation changes of the polysaccharide rendering the CD-moieties inaccessible for the polymer probe, will be not of primary importance. However, the presence of polymeric components, for example, in the form of adamantane-poly(ethylene glycol), seems to have a strong effect on the equilibrium constant of the AD/CD inclusion complex.⁶⁹ In their presence, even irreversible association of AD/CD complexes has been observed with respect to rinsing with water.^{73,74}

The interpretation that the reduced adhesion for the CHI-AD polymer probe and CHI-CDBlocked has to be attributed to the blocking or inaccessibility of the CD-moieties is further confirmed by the adhesion behavior of the same polymer probe with an unmodified chitosan layer. In this case, the adhesion is primarily characterized by a small jump-out of contact directly after separation of the surfaces, which originates from the contact area between tip and sample (cf., Figure 3c). In the case of the CHI-CDBlocked, the small number of observed events might be attributed to incomplete blocking or dissociated host–guest complexes in the solution free of AD-COOH. In the following paragraphs, we will further analyze the difference in adhesion behavior for the different samples on a quantitative level.

Quantitative Analysis of the Adhesion Behavior. For a quantitative description of the interaction between the different chitosan layers, we analyzed in detail the retraction profiles between the polymer probe and the layers immobilized to the flat surface. The first part of this quantitative analysis is based on the occurrence of rupture events at the single polymer level. For each combination of polymer probe and chitosan layer, a statistically

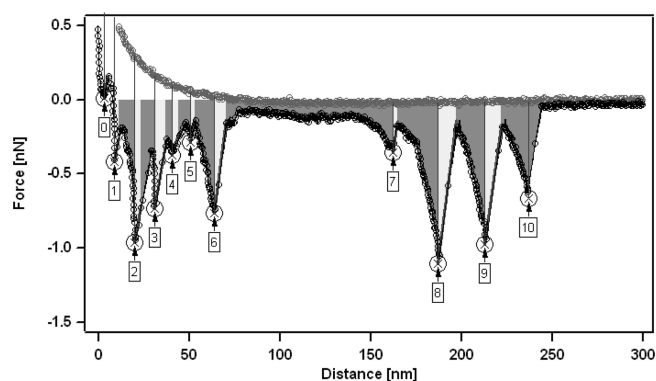


Figure 4. A representative force profile with various rupture events. The boxed numbers indicate the rupture events as those identified by the detection algorithms. Additionally, the area below the force curve obtained by integration is shaded in gray. The light gray areas, which are included in the total area, correspond to cantilever instabilities following a rupture event.

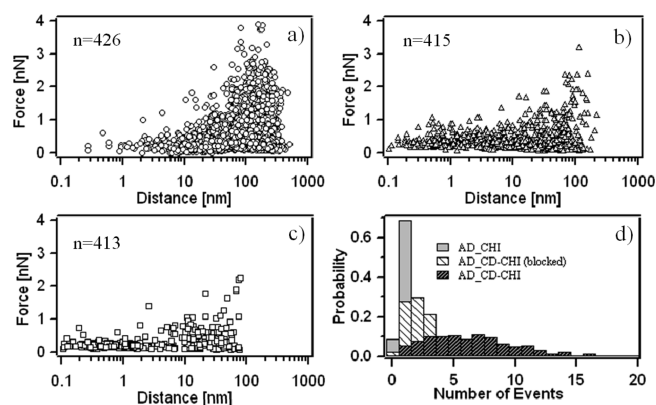


Figure 5. Scatter plots of the detachment force versus corresponding separation distance obtained with a polymer probe (CHI-AD) against (a) CHI-CD, (b) CHI-CDBlocked, and (c) CHI. The number n of force profiles from which the plots have been compiled is approximately equal. The distribution of the average number of detachment events per profile for the various chitosan derivatives is represented in (d).

relevant number of force profiles (>100 curves) were acquired at one position. At least four different positions were measured for each sample. The resulting data sets of force profiles for one polymer probe versus various surfaces (>2000 curves) have been analyzed by means of an automated algorithm, which used a constant set of parameters for the whole data set.^{31,32,75} Figure 4 gives an example that demonstrates the extracted data from each force profile.

In Figure 4 are indicated the rupture events on the single molecule level as identified by the aforementioned algorithm. As all of these events correspond to the detachment of one or more polymer segments, their occurrence is erratic and reflects the variation in polymer segment length as well as in the detachment and unbinding force. Therefore, number and position of these events vary even for force profiles taken at the same sample position. To provide an overall assessment or “fingerprinting” of the adhesion behavior between the different chitosan layers, we summarize all events determined for the chitosan layers on the probe and sample in one scatter plot (cf., Figure 5a–c). These scatter plots show the critical force where detachment occurred as a function of the corresponding separation distance and each

event is presented by a separate point. A similar approach in plotting the adhesion forces has been presented in the past for the adhesion for various polymeric systems, such as the adhesion in synthetic polyelectrolyte layers or the adhesion in biopolymer systems.^{32,76}

A number of different parameters are considered as indicative for the various aspects of the adhesion process. The total number of events per curve (cf., Figure 5d) is one of these parameters. This quantity is strongly correlated to the total number of polymer segments bridged between the two surfaces.⁶⁶ A second indicator is the separation distance at which the last detachment event occurs for each force curve; this distance reflects the length of the longest polymer segment bridged between the surfaces.⁶⁸ Both values have been compiled in Table 1 for the different probe versus sample combinations. Furthermore, we calculated the area enclosed between the line of zero force and the force profile upon retraction. This area, indicated in gray in Figure 4, corresponds in an approximate manner to the work of adhesion, which is the work necessary to separate the polymer probe from the surface.^{31,32,77} We will discuss the work of adhesion below in detail, as it represents a measure for the overall interactions on the molecular level.

Comparison of the Adhesion Behavior. The scatter plots represented in Figure 5a–c summarize the adhesion behavior for one polymer probe (CHI-AD) against different chitosan layers (CHI-CD, CHI-CDBlocked, and CHI, respectively). All scatter plots are compiled from approximately the same number of force profiles. For a given polymer probe, no significant variation of these distributions has been observed within a series of force curves at the same position or upon variation of the lateral sample position on the same sample. However, each polymer probe results in a unique distribution of detachment events as the length and the number of protruding CHI-AD segments vary between the different polymer probes. Nevertheless, the differences between the different samples in terms of above indicators (number of events, separation distance of last event, and work of adhesion) were observed when conducting experiments with different polymer probes and various samples.

Comparison of the scatter plots for the different combinations of chitosan shows clear trends for the separation distances and corresponding forces for the rupture events. Only the combination of probe and sample that allows for host–guest interactions (i.e., CHI-AD vs CHI-CD, cf., Figure 5a) leads to a significant number of rupture events taking place at large separation distances above 100 nm. At these distances larger forces are observed, which might result from the simultaneous rupture of several AD/CD-complexes. Instead, for the blocked CD-modified surface (CHI-AD vs CHI-CDBlocked, Figure 5b) or the bare chitosan surface (CHI-AD vs CHI, Figure 5c), practically all rupture events are taking place at separations below 100 nm. A strong indicator for the differences in the adhesion is the separation of the last detachment event per force profile, which corresponds to the length of the longest polysaccharide element bridged (cf., Table 1). The average separation distance for the last detachment event for CHI-AD versus CHI is 8 nm and for CHI-AD versus CHI-CDBlocked it is about 31 nm, respectively. Instead, for CHI-AD versus CHI-CD, one finds an average separation distance of about 185 nm for the last detachment event. Therefore, only in the presence of host–guest interactions is the bridging of sufficiently long chitosan strands occurring.

For the combination CHI-AD versus CHI-CD, the distances of detachment are not equally distributed but cluster instead at

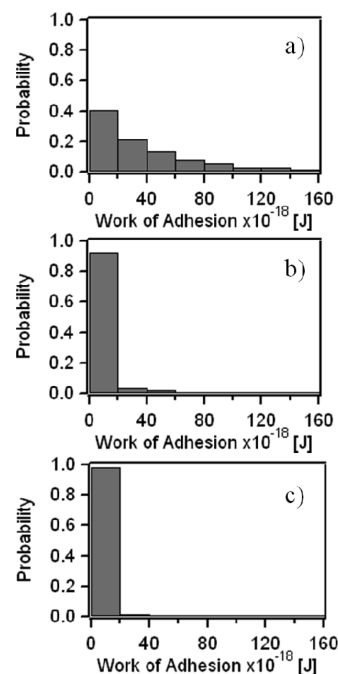
Table 1. Parameters Describing the Adhesive Behavior of a Polymer Probe with CHI-AD against Various Chitosan Layers

surfaces versus AD-polymer probe	separation distance of last event (nm)	number of events	work of adhesion ($\times 10^{-18}$ J)
CHI-CD	185 ± 98	7 ± 4	47 ± 59
CHI-CD _{blocked}	31 ± 34	3 ± 2	7 ± 15
CHI	8 ± 16	1 ± 1	2 ± 4

large distances. This shift to large separations results from the formation of host–guest complexes between the polymer strands. Certainly, the number of polymer/polymer contacts is largest in the contact area. However, the number of cyclodextrin hosts inside this contact area is limited. Even for densest possible hexagonal packing, only about 40 CD moieties would find place in a contact area of 100 nm^2 . For the formation of AD/CD-complexes, only a small fraction of these would be accessible due to steric constraints, as the polymer density in the contact area is very high. Instead, longer polymer segments can access a large sample area where the AFM-tip is not in direct contact with the sample to form additional bonds. Those bonds will rupture consequently at large separation distances. The strong dependence of the number of events with increasing contact time is a further indication for this process. The molecular mass of the chitosan (372 kDa) corresponds to a contour length of 2485 nm. On the basis of a Kuhn length of 22 nm for chitosan, which represents an approximate average of values found in the literature,^{37,39} and this molecular mass, we obtain a radius of gyration R_g of 95 nm. An average distance of 185 nm for the last rupture event seems in this respect reasonable (cf., Figure 5b).

The average number of rupture events per curve is probably the most significant indicator for host–guest interactions between the polymer probe (CHI-AD) and the chitosan bearing cyclodextrin units (CHI-CD). The observed average value of 7 ± 4 events is significantly higher than the averages of 1 ± 1 and 3 ± 2 for the interaction of same polymer probe with CHI and CHI-CD_{blocked} layers, respectively. For the latter two layers, only unspecific interactions are expected. The higher number of events for the interaction between blocked CHI-CD in comparison to the bare chitosan can be attributed to the presence of previously unblocked cyclodextrin units or to the kinetic unbinding during the measurement in the solution that does not contain 1-adamantanecarboxylic acid (AD-COOH). The blocking of CD cavities was performed under basic conditions (pH 8) due to the very low solubility of adamantanecarboxylic acid (pK_a 5) at low pH. Although the measurements were performed in the standard buffer (pH 3.7) and the solubility of adamantanecarboxylic acid is dramatically decreased in acidic conditions, this solubility hindrance might have prevented the complete dissociation of inclusion complexes of AD-COOH/CD.

The 7 ± 4 events per curve for CHI-AD versus CHI-CD is compatible with the estimated number of adamantane (AD) units per polymer strand. Given an average detachment distance for the last event of about 185 nm, one can expect approximately 13 guests (AD) on a chitosan strand of this length. Although multiple CHI-AD strands, albeit of shorter length, might bind within a circle of this radius, the formation of host–guest complexes will be possible only in a fraction of cases due to steric constraints. In future studies, we intend to vary the grafting density of the CD-moieties on the surface, to experimentally verify this hypothesis further.

**Figure 6.** Work of adhesion obtained by integrating the area enclosed by the retraction force profile and the x -axis (cf., Figure 4) for the same polymer probe (CHI-AD) interacting with (a) CHI-CD, (b) CHI-CD_{blocked}, and (c) an unmodified chitosan (CHI) layer.

Interactions on the Molecular Level and Total Work of Adhesion. The scatter plots in Figure 5 indicate a variation of the average rupture forces for the different chitosan derivatives. One finds the average detachment force for the CHI-CD layer at 0.54 nN, in comparison to 0.30 nN for the bare chitosan (CHI), and 0.39 nN for CHI-CD_{blocked}. These average values are significantly larger than the reported unbinding force of 102 ± 15 pN, for the host/guest interaction between adamantane and β -cyclodextrin.²⁶ However, it should be noticed that the detachment forces differ not significantly for the chitosan layers where host–guest complex formation is possible from those where it is not possible. Therefore, we assume that nonspecific interactions play also an important role for the detachment processes between two chitosan strands, independent from their chemical modification by additional moieties. Furthermore, the complex unbinding topology due to the presence of multiple host–guest complexes on the polysaccharide backbone can have a significant influence on the determined unbinding force. In particular, the presence of one AD molecule at every ~ 14 nm on the chitosan allows for the simultaneous rupture of more than one host–guest complex. Because of these uncertainties, a quantitative approach, which takes into account the properties of an ensemble of host–guest complexes linked to polymeric spacers, has to be applied to describe the detachment of the CD/AD-complexes quantitatively.⁷⁸ However, such a quantitative evaluation is out the scope of this study.

The various contributions on the molecular level to the adhesion between the chitosan strands can be summarized by the work of adhesion. The work of adhesion W is defined here as $W = \int F(z) dz$, where z is the separation distance and $F(z)$ is the force at separation z . W is obtained by determining the total area between the line of zero force (i.e., x -axis) and the force profile upon retraction (the gray area in Figure 4). A similar approach

has been proposed previously by various groups.^{31,32,77,79} The distributions of the work of adhesion for the different surfaces are presented in Figure 6. The average work of adhesion is 47×10^{-18} , 7×10^{-18} , and 2×10^{-18} J for the AD-polymer probe against CHI-CD (cf., Figure 6a), CHI-CD_{blocked} (cf., Figure 6b), and CHI (cf., Figure 6c), respectively. Thus, the formation of host–guest complexes leads to an about 10 times higher work to separate the surfaces than in its absence. The work of adhesion does not only reflect the enthalpic contribution to unbind the host–guest complexes but also the work due to the additional stretching of the polymer segments, which are connected due to these inclusion complexes. The former contributions are characterized by the area enclosed by the instabilities of the cantilever (light gray area in Figure 4). These instabilities result from rupture of previously bonded polymer strands and lead to an instantaneous “snapping-back” of cantilever in the direction of its zero deflection. During this movement, the force profile is practically linear with a slope equaling the spring constant of the cantilever. The fraction of the area under the force curve that can be attributed to the instabilities following the unbinding events represents about 10–40% in the case of CHI-AD versus CHI-CD for the large majority of the curves. However, due to the cantilever instability, a direct attribution of the work of adhesion to each rupture event is not practicable. Furthermore, these rupture events will often result from breaking more than one AD/CD inclusion complex simultaneously and are not constricted in their pulling geometry due the attachment of hosts as well as guests to a polymeric chain.

CONCLUSIONS

Polymer probes, which are obtained by the modification of a small AFM-tip with protruding polymer segments, allow one to determine the interaction between few polymer strands. By this technique, the main contributions to the interaction between modified chitosan layers could be identified. In particular, the work of adhesion, that is, the work necessary to separate the polysaccharide layers, is about an order of magnitude larger for those chitosan derivatives that can form host–guest complexes than for those where this is not possible.

By introducing multivalent binding on the base of supra-molecular interactions into the adhesion process between the polysaccharide layers, the adhesion between the layers can be tuned in a defined manner. The here-proposed method allows in principle separating two contributions to the total work of adhesion: the enthalpic rupture of host–guest interactions and the entropic stretching of the polysaccharide chains at the molecular level. The here-examined modified chitosans are therefore not only very promising in terms of their potential for future applications, such as switchable coatings, but also represent a versatile model system to follow the adhesion in polyelectrolyte layers at the molecular level, for example, by varying the grafting density of the host and guest moieties on the polysaccharide backbone.

ASSOCIATED CONTENT

S Supporting Information. Surface topography of chitosan-modified surfaces and reproducibility of adhesion behavior as obtained by the polymer probe. This material is available free of charge via the Internet at <http://pubs.acs.org>.

AUTHOR INFORMATION

Corresponding Author

*E-mail: georg.papastavrou@uni-bayreuth.de (G.P.); andreas.fery@uni-bayreuth.de (A.F.).

ACKNOWLEDGMENT

O.K. and A.F. acknowledge the financial support from European Community Collaborative Project 3MICRON within call FP7-NMP-2009-LARGE-3. S.T. and G.P. acknowledge the support by COST D-33 and the Swiss State Secretariat for Research and Technology. Furthermore, we thank P. Maroni (University of Geneva) and C. Kuttner (University of Bayreuth) for help with the ellipsometric measurements.

REFERENCES

- (1) Charlot, A.; Auzely-Velty, R.; Rinaudo, M. *J. Phys. Chem. B* **2003**, *107*, 8248–8254.
- (2) Charlot, A.; Auzely-Velty, R. *Macromolecules* **2007**, *40*, 1147–1158.
- (3) Falvey, P.; Lim, C. W.; Darcy, R.; Revermann, T.; Karst, U.; Giesbers, M.; Marcelis, A. T. M.; Lazar, A.; Coleman, A. W.; Reinhoudt, D. N.; Ravoo, B. J. *Chem.-Eur. J.* **2005**, *11*, 1171–1180.
- (4) Ravoo, B. J.; Jacquier, J.-C.; Wenz, G. *Angew. Chem.* **2003**, *115*, 2112–2116.
- (5) Van der Heyden, A.; Wilczewski, M.; Labbe, P.; Auzely, R. *Chem. Commun.* **2006**, 3220–3222.
- (6) Suzuki, I.; Egawa, Y.; Mizukawa, Y.; Hoshi, T.; Anzai, J. *Chem. Commun.* **2002**, 164–165.
- (7) Crespo-Biel, O.; Ravoo, B. J.; Reinhoudt, D. N.; Huskens, J. *J. Mater. Chem.* **2006**, *16*, 3997–4021.
- (8) Crespo-Biel, O.; Ravoo, B. J.; Huskens, J.; Reinhoudt, D. N. *Dalton Trans.* **2006**, 2737–2741.
- (9) Uhlenheuer, D. A.; Petkau, K.; Brunsveld, L. *Chem. Soc. Rev.* **2010**, *39*, 2817–26.
- (10) Mammen, M.; Choi, S.-K.; Whitesides, G. M. *Angew. Chem., Int. Ed.* **1998**, *37*, 2754–2794.
- (11) Gestwicki, J. E.; Cairo, C. W.; Strong, L. E.; Oetjen, K. A.; Kiessling, L. L. *J. Am. Chem. Soc.* **2002**, *124*, 14922–14933.
- (12) Mulder, A.; Huskens, J.; Reinhoudt, D. N. *Org. Biomol. Chem.* **2004**, *2*, 3409–3424.
- (13) Gargano, J. M.; Ngo, T.; Kim, J. Y.; Acheson, D. W. K.; Lees, W. J. *J. Am. Chem. Soc.* **2001**, *123*, 12909–12910.
- (14) Huskens, J.; Mulder, A.; Auletta, T.; Nijhuis, C. A.; Ludden, M. J. W.; Reinhoudt, D. N. *J. Am. Chem. Soc.* **2004**, *126*, 6784–6797.
- (15) Huskens, J. *Curr. Opin. Chem. Biol.* **2006**, *10*, 537–543.
- (16) Mulder, A.; Auletta, T.; Sartori, A.; Del Ciotto, S.; Casnati, A.; Ungaro, R.; Huskens, J.; Reinhoudt, D. N. *J. Am. Chem. Soc.* **2004**, *126*, 6627–6636.
- (17) Janshoff, A.; Neitzert, M.; Oberdorfer, Y.; Fuchs, H. *Angew. Chem., Int. Ed.* **2000**, *39*, 3213–3237.
- (18) Frago, A.; Caballero, J.; Almirall, E.; Villalonga, R.; Cao, R. *Langmuir* **2002**, *18*, 5051–5054.
- (19) Florin, E. L.; Moy, V. T.; Gaub, H. E. *Science* **1994**, *264*, 415–417.
- (20) Moy, V. T.; Florin, E. L.; Gaub, H. E. *Science* **1994**, *266*, 257–259.
- (21) Wong, J.; Chilkoti, A.; Moy, V. T. *Biomol. Eng.* **1999**, *16*, 45–55.
- (22) Dufrene, Y. F.; Hinterdorfer, P. *Pfluegers Arch.: Eur. J. Physiol.* **2008**, *456*, 237–245.
- (23) Wong, J. Y.; Kuhl, T. L.; Israelachvili, J. N.; Mullah, N.; Zalipsky, S. *Science* **1997**, *275*, 820–822.
- (24) Hinterdorfer, P.; Gruber, H. J.; Kienberger, F.; Kada, G.; Riener, C.; Borken, C.; Schindler, H. *Colloids Surf., B* **2002**, *23*, 115–123.

- (25) Jeppesen, C.; Wong, J. Y.; Kuhl, T. L.; Israelachvili, J. N.; Mullah, N.; Zalipsky, S.; Marques, C. M. *Science* **2001**, 293, 465–468.
- (26) Auletta, T.; de Jong, M. R.; Mulder, A.; van Veggel, F.; Huskens, J.; Reinhoudt, D. N.; Zou, S.; Zapotoczny, S.; Schonherr, H.; Vancso, G. J.; Kuipers, L. *J. Am. Chem. Soc.* **2004**, 126, 1577–1584.
- (27) Schonherr, H.; Beulen, M. W. J.; Bugler, J.; Huskens, J.; van Veggel, F.; Reinhoudt, D. N.; Vancso, G. J. *J. Am. Chem. Soc.* **2000**, 122, 4963–4967.
- (28) Claesson, P. M.; Poptoshev, E.; Blomberg, E.; Dedinaite, A. *Adv. Colloid Interface Sci.* **2005**, 114–115, 173–187.
- (29) Blomberg, E.; Poptoshev, E.; Claesson, P. M.; Caruso, F. *Langmuir* **2004**, 20, 5432–5438.
- (30) Blomberg, E.; Poptoshev, E.; Caruso, F. *Langmuir* **2006**, 22, 4153–4157.
- (31) Kirwan, L. J.; Maroni, P.; Behrens, S. H.; Papastavrou, G.; Borkovec, M. *J. Phys. Chem. B* **2008**, 112, 14609–14619.
- (32) Pericet-Camara, R.; Papastavrou, G.; Behrens, S. H.; Helm, C. A.; Borkovec, M. *J. Colloid Interface Sci.* **2006**, 296, 496–506.
- (33) Bosio, V.; Dubreuil, F.; Bogdanovic, G.; Fery, A. *Colloids Surf., A* **2004**, 243, 147–155.
- (34) Takemasa, M.; Sletmoen, M.; Stokke, B. T. *Langmuir* **2009**, 25, 10174–10182.
- (35) Dubacheva, G. V.; Dumy, P.; Auzely, R.; Schaaf, P.; Boulmedais, F.; Jierry, L.; Coche-Guerente, L.; Labbe, P. *Soft Matter* **2010**, 6, 3747–3750.
- (36) Mourya, V. K.; Inamdar, N. N. *React. Funct. Polym.* **2008**, 68, 1013–1051.
- (37) Mazeau, K.; Perez, S.; Rinaudo, M. *J. Carbohydr. Chem.* **2000**, 19, 1269–1284.
- (38) Morris, G. A.; Castile, J.; Smith, A.; Adams, G. G.; Harding, S. E. *Carbohydr. Polym.* **2009**, 76, 616–621.
- (39) Brugnerotto, J.; Desbrieres, J.; Roberts, G.; Rinaudo, M. *Polymer* **2001**, 42, 9921–9927.
- (40) Alves, N. M.; Mano, J. F. *Int. J. Biol. Macromol.* **2008**, 43, 401–414.
- (41) Rekharsky, M. V.; Inoue, Y. *Chem. Rev.* **1998**, 98, 1875–1917.
- (42) Evans, E.; Ritchie, K. *Biophys. J.* **1997**, 72, 1541–1555.
- (43) Merkel, R.; Nassoy, P.; Leung, A.; Ritchie, K.; Evans, E. *Nature* **1999**, 397, 50–53.
- (44) Hugel, T.; Grosholz, M.; Clausen-Schaumann, H.; Pfau, A.; Gaub, H.; Seitz, M. *Macromolecules* **2001**, 34, 1039–1047.
- (45) Friedsam, C.; Gaub, H. E.; Netz, R. R. *Biointerphases* **2006**, 1, MR1–MR21.
- (46) Seitz, M.; Friedsam, C.; Jostl, W.; Hugel, T.; Gaub, H. E. *ChemPhysChem* **2003**, 4, 986–990.
- (47) Auzely-Velty, R.; Rinaudo, M. *Macromolecules* **2002**, 35, 7955–7962.
- (48) Charlot, A. Ph.D. Dissertation, Université Joseph Fourier, Grenoble I, France, 2005.
- (49) Charlot, A.; Heyraud, A.; Guenot, P.; Rinaudo, M.; Auzely-Velty, R. *Biomacromolecules* **2006**, 7, 907–913.
- (50) Auzély, R.; Rinaudo, M. *Macromol. Biosci.* **2003**, 3, 562–565.
- (51) Auzely-Velty, R.; Rinaudo, M. *Macromolecules* **2001**, 34, 3574–3580.
- (52) Rinaudo, M.; Milas, M.; Dung, P. L. *Int. J. Biol. Macromol.* **1993**, 15, 281–285.
- (53) Kern, W.; Puotinen, D. A. *RCA Rev.* **1970**, 31, 187–206.
- (54) Schauer, C. L.; Chen, M.-S.; Chatterley, M.; Eisemann, K.; Welsh, E. R.; Price, R. R.; Schoen, P. E.; Ligler, F. S. *Thin Solid Films* **2003**, 434, 250–257.
- (55) Hutter, J. L.; Bechhoefer, J. *Rev. Sci. Instrum.* **1993**, 64, 1868–1873.
- (56) Sader, J. E.; Chon, J. W. M.; Mulvaney, P. *Rev. Sci. Instrum.* **1999**, 70, 3967–3969.
- (57) Auletta, T.; Dordi, B.; Mulder, A.; Sartori, A.; Onclin, S.; Bruinink, C. M.; Péter, M.; Nijhuis, C. A.; Beijleveld, H.; Schönherr, H.; Vancso, G. J.; Casnati, A.; Ungaro, R.; Ravoo, B. J.; Huskens, J.; Reinhoudt, D. N. *Angew. Chem., Int. Ed.* **2004**, 43, 369–373.
- (58) Huskens, J.; Deij, M. A.; Reinhoudt, D. N. *Angew. Chem., Int. Ed.* **2002**, 41, 4467–4471.
- (59) Luzinov, I.; Julthongpiput, D.; Liebmann-Vinson, A.; Cregger, T.; Foster, M. D.; Tsukruk, V. V. *Langmuir* **2000**, 16, 504–516.
- (60) Trimbach, D. C.; Keller, B.; Bhat, R.; Zankovych, S.; Pohlmann, R.; Schroter, S.; Bossert, J.; Jandt, K. D. *Adv. Funct. Mater.* **2008**, 18, 1723–1731.
- (61) Chao, A. C. J. *Membr. Sci.* **2008**, 311, 306–318.
- (62) Kallury, K. M. R.; Macdonald, P. M.; Thompson, M. *Langmuir* **1994**, 10, 492–499.
- (63) Wong, A. K. Y.; Krull, U. J. *Anal. Bioanal. Chem.* **2005**, 383, 187–200.
- (64) Schneider, A.; Picart, C.; Senger, B.; Schaaf, P.; Voegel, J.-C.; Frisch, B. *Langmuir* **2007**, 23, 2655–2662.
- (65) Israelachvili, J. N. *Intermolecular and Surface Forces*; Academic Press: London, 1991.
- (66) Marszalek, P. E.; Li, H. B.; Fernandez, J. M. *Nat. Biotechnol.* **2001**, 19, 258–262.
- (67) Giannotti, M. I.; Vancso, J. G. *ChemPhysChem* **2007**, 8, 2290–2307.
- (68) Papastavrou, G.; Kirwan, L. J.; Borkovec, M. *Langmuir* **2006**, 22, 10880–10884.
- (69) Poon, K. H. N.; Cheng, Y. L. *J. Inclusion Phenom. Macrocyclic Chem.* **2008**, 60, 211–222.
- (70) de Jong, M. R.; Huskens, J.; Reinhoudt, D. N. *Chem.-Eur. J.* **2001**, 7, 4164–4170.
- (71) Soto Tellini, V. H.; Jover, A.; Garcia, J. C.; Galantini, L.; Meijide, F.; Tato, J. V. *J. Am. Chem. Soc.* **2006**, 128, 5728–5734.
- (72) Kwak, E.; Gomez, F. *Chromatographia* **1996**, 43, 659–662.
- (73) Kham, K.; Guerrouache, M.; Carbonnier, B.; Lazerges, M.; Perrot, H.; Millot, M. C. *J. Colloid Interface Sci.* **2007**, 315, 800–804.
- (74) David, C.; Millot, M. C.; Sébille, B. *J. Chromatogr., B: Biomed. Sci. Appl.* **2001**, 753, 93–99.
- (75) Gergely, C.; Senger, B.; Voegel, J. C.; Hörber, J. K. H.; Schaaf, P.; Hemmerlé, J. *Ultramicroscopy* **2000**, 87, 67–78.
- (76) Abu-Lail, N. I.; Camesano, T. A. *J. Microsc.* **2003**, 212, 217–238.
- (77) Weder, G.; Voros, J.; Giazson, M.; Matthey, N.; Heinzlmann, H.; Liley, M. *Biointerphases* **2009**, 4, 27–34.
- (78) Guo, S.; Ray, C.; Kirkpatrick, A.; Lad, N.; Akhremitchev, B. B. *Biophys. J.* **2008**, 95, 3964–3976.
- (79) Weder, G.; Blondiaux, N.; Giazson, M.; Matthey, N.; Klein, M.; Pugin, R.; Heinzlmann, H.; Liley, M. *Langmuir* **2010**, 26, 8180–8186.